IOPscience iopscience.iop.org

Home Search Collections Journals About Contact us My IOPscience

MR damper based implementation of nonlinear damping for a pitch plane suspension system

This content has been downloaded from IOPscience. Please scroll down to see the full text.

2012 Smart Mater. Struct. 21 045006

(http://iopscience.iop.org/0964-1726/21/4/045006)

View the table of contents for this issue, or go to the journal homepage for more

Download details:

IP Address: 137.30.242.61
This content was downloaded on 30/06/2014 at 07:39

Please note that terms and conditions apply.

Smart Mater. Struct. **21** (2012) 045006 (14pp) doi:10.1088/0964-1726/21/4/045006

MR damper based implementation of nonlinear damping for a pitch plane suspension system

H Laalej[1], **Z Q Lang**[1], **B Sapinski**[2] **and P Martynowicz**[2]

[1] Department of Automatic Control and Systems Engineering, University of Sheffield, Mapping Street, Sheffield S1 3JD, UK
[2] Department of Process Control, AGH University of Science and Technology, aleja Mickiewicza 30, 30-059 Cracow, Poland

E-mail: z.lang@shef.ac.uk and deep@agh.edu.pl (Sapinski)

Received 22 June 2011, in final form 19 February 2012
Published 14 March 2012
Online at stacks.iop.org/SMS/21/045006

Abstract
Suppression of vibration transmission from working machineries and other sources is important for the normal operation of a wide range of engineering systems. Traditionally, viscous dampers with approximately linear characteristics are often used to address the issue. However, this solution can have the problem of not being able to reduce the vibration transmission over the whole range of frequencies. In recent studies, the authors have revealed, by both theoretical analysis and experimental test, that nonlinear damping can be applied to resolve the problem. The present study is concerned with the exploitation of this beneficial effect of nonlinear damping to the vibration control of a pitch plane suspension system. A magneto-rheological (MR) damper based implementation of nonlinear damping is applied to provide a novel solution to the pitch plane system vibration control problem. Simulation studies are conducted to demonstrate the effectiveness of the MR damper implementation, and the beneficial effect of nonlinear damping on the pitch plane suspension system vibration control.

(Some figures may appear in colour only in the online journal)

1. Introduction

Vibration transmitted from working machinery and other sources such as propulsion engines, diesel generators, air compressors, and bumping roads, etc can cause problems in a wide range of applications [1–5]. In order to address this issue, viscous dampers with approximately linear characteristics have been widely used as isolation devices to reduce the adverse effect of vibration. However, this technique is sometimes not very effective. It is well known that as the level of linear viscous damping is increased in order to reduce the force transmissibility over the resonant frequency region of a vibrating system, the transmissibility over higher frequency regions will be increased [6, 7]. This phenomenon produces a dilemma associated with the design of linear viscously damped vibration isolation systems.

In order to resolve the problem, the use of nonlinear damping has been considered since 1970's [8]. Recently, the authors introduced a cubic nonlinear damping into a single-degree of freedom (sdof) vibrating system and theoretically proved that the cubic nonlinear damping can reduce the force transmissibility over the system resonant frequency region, whilst keeping the transmissibility over other frequency regions almost unaffected [9]. The theoretical conclusions were then verified by experimental tests on a vibration isolation mount [10] where electrodynamic shakers were used to actively implement a desired cubic nonlinear damping characteristic. In a further study [11], these conclusions have been extended to multi-degree of freedom (mdof) lumped parameter systems. The results show that a cubic nonlinear damping can reduce the system force transmissibility around all resonant frequency regions but has

 © 2012 IOP Publishing Ltd Printed in the UK & the USA

almost no effect on the transmissibility over non-resonant frequency regions. These studies demonstrate the benefits and feasibility of exploitation of nonlinear damping to more effectively address a wide range of vibration control problems.

The pitch plane suspension system is a physical model of vehicle seat suspension systems. The system has been widely used by researchers to study the behaviour of vehicles, particularly off-road vehicles, where the vibration control objective is to reduce the vertical force transmitted from the unevenness of terrain, driving speed, loading, and driving style, etc to the driver seat [12]. This transmitted force cannot only reduce the working efficiency of drivers but also has a significant impact on the drivers' health, as it causes stress to joint and spine and results in driver backache [12]. Traditionally, this problem was tackled using a passive solution, e.g. placing an elastomeric rubber between the driver seat and the frame of a vehicle. This is, however, not very effective. It was found that drivers can still be subjected to vibration levels that exceed the ISO exposure limits [13, 14]. To resolve this problem, considerable research studies have been devoted to developing new methods capable of reducing the force transmitted to the driver. These efforts have resulted in the development of semi-active solutions, particularly MR damper based techniques [15–17].

MR dampers are semi-active damping devices whose damping characteristic can be changed by a control current. The control current only changes the damping properties of MR dampers; there is no energy input into vibrating systems. However, the relationship between the MR damper control current and damping force is nonlinear. This makes the MR damper based vibration control a challenging task. To overcome this problem, researchers have developed different feedback control systems to address this issue. For example, Chang and Zhou [18] used a neural network to emulate the inverse dynamics of a MR damper, showing that the MR damper can be commanded to achieve a desired control. In another study, Zhou and Chang [19] developed an adaptive fuzzy controller to minimize the difference between the desired and the actual structural response where a MR damper was used to implement the control action. Dyke *et al* [20] proposed a clipped optimal control based on the acceleration feedback where a MR damper was applied to realize the desired optimal control. In most currently available MR damper based vibration control techniques, including those proposed for pitch plane suspension systems, the MR damper was used like an actuator in a standard feedback control system. In the system, the desired response is compared with the actual response; the resulting error is fed into a controller which generates a control signal that drives MR control current to produce a corresponding MR damper resistance force to compensate for the effect of vibrations from ambient disturbances on the system.

Given the dissipative nature of MR damping devices, the authors think that in many applications, a more effective use of MR dampers would be to directly use them as dampers rather than as actuators in a feedback control loop, and exploit the MR damper control current to achieve a desired damping characteristic. This idea has already been adopted in [21] where a feedback control approach was proposed to shape the force/velocity response of MR dampers as needed. However, as far as we are aware, there was still no application of a MR damper with a purposely shaped nonlinear damping characteristic to literally achieve a desired vibration control. This is probably because the beneficial effects of nonlinear damping on vibration control have not been fully realized in relevant areas.

The present study is concerned with exploiting the beneficial effects of nonlinear damping revealed in [9–11] to conduct the vibration control of an experimental pitch plane suspension system. An MR damper is used in the system to realize a desired cubic nonlinear damping characteristic via a feedback control of the MR damper resistance force. This approach directly uses the MR damper as a damper rather than an actuator in a feedback control loop to address a vibration control issue, and provides a novel solution to a well-known vibration control problem.

In this paper, the mathematical model of the experimental pitch plane suspension system with fitted MR dampers is first derived. The nonparametric model proposed by Song *et al* in [22] is used to represent the MR dampers in the model. A feedback control is then introduced to shape the damping curve of the MR damper fitted under the cabin/seat of the system to achieve a desired cubic nonlinear damping characteristic. After that, the performance of the novel MR damper based pitch plane suspension system vibration control is investigated by simulation studies. These results establish the principle and demonstrate the effectiveness of the proposed novel solution to pitch plane suspension system vibration control problems, and provide a necessary basis for future experimental studies.

2. Modelling of a pitch plane suspension system with fitted MR dampers

2.1. Pitch plane suspension system

The pitch plane suspension system considered in the present study is shown in figure 1. This system comprises a stiff beam of mass m_t simulating a vehicle frame and a rigid body of mass m_s representing the cabin or seat of the vehicle. The beam is supported by a MR damper and a parallel spring at point P_f (front of the vehicle) and P_r (rear of the vehicle), respectively. The stiffness coefficients of the front and rear spring are denoted by k_f and k_r. The rigid body is suspended at point P_s by a spring with stiffness k_s in parallel with another MR damper d_s. The movement of the rigid body is restricted to be perpendicular to the beam. This setup represents the practical situation where MR dampers are fitted in the front and rear suspension systems and underneath the driver seat of a vehicle.

The system has three degrees of freedom (3dof), which are the vertical displacement $x_t(t)$ of the beam's centre-of-gravity (P_g), the beam's pitch (rotation) angle $\varphi(t)$, and the relative displacement $\delta_s(t)$ of the rigid body m_s in the direction perpendicular to the beam. When the system is subjected to a kinetic type excitation $w_f(t)$ at the front

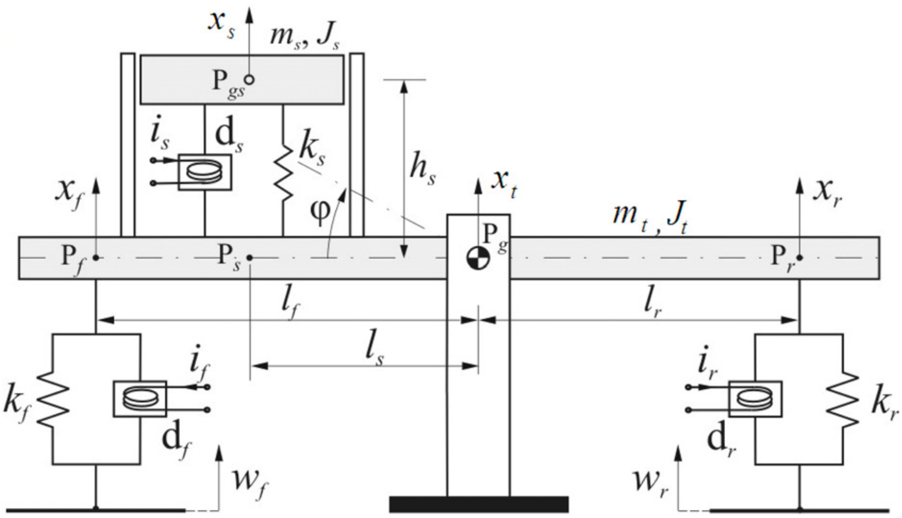

Figure 1. A pitch plane suspension system with fitted MR dampers.

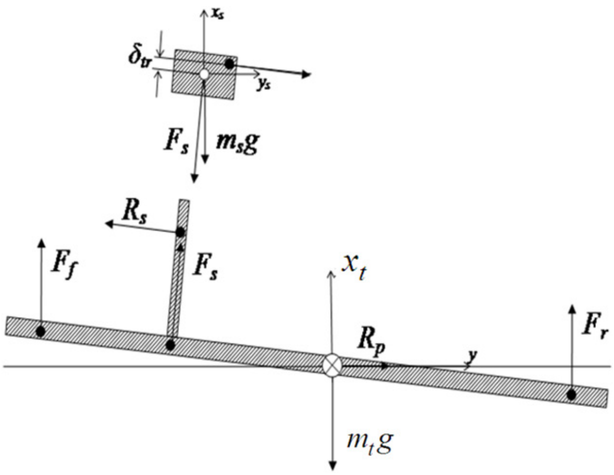

Figure 2. Free-body diagram of the pitch plane suspension system.

suspension, vertical displacements $x_f(t)$ and $x_r(t)$ are produced at points P_f and P_r, transmitting a undesired force $m_s\ddot{x}_s(t)$ to the seat where

$$x_s(t) = x_t(t) + l_s\sin(\varphi(t)) + \delta_s(t)\cos(\varphi(t)) \tag{1}$$

represents the absolute displacement of mass m_s.

Denote

$$\delta_r(t) = x_t(t) - l_r\sin(\varphi(t)) - w_r(t) = x_t(t) - l_r\sin(\varphi(t)) \tag{2}$$

$$\begin{aligned}\delta_f(t) &= x_t(t) + l_f\sin(\varphi(t)) - w_f(t)\\ &= x_t(t) + l_f\sin(\varphi(t)) - w_f(t)\end{aligned} \tag{3}$$

and assume $w_r(t) = 0$ in this study. Additionally, it is assumed that the rolling frictions in the guiding mechanisms of the beam's centre-of-gravity and beam/body suspension-sets are negligible.

Figure 2 shows the free-body diagram of the system, where R_s and R_p denote the resultant reactions of the rigid body and the beam's centre-of-gravity guiding mechanism, respectively.

By using the d'Alembert principle, the system dynamic equations can be obtained as

$$\begin{aligned}
0 &= -m_t\ddot{x}_t(t) - k_f\delta_f(t) - k_r\delta_r(t) + k_s\delta_s(t)\cos(\varphi(t)) - F_{df}(t)\\
&\quad - F_{dr}(t) + F_{ds}(t)\cos(\varphi(t)) + R_s\sin(\varphi(t)) - m_t g\\
0 &= -J_t\ddot{\varphi}(t) - k_f l_f\delta_f(t)\cos(\varphi(t)) + k_r l_r\delta_r(t)\cos(\varphi(t))\\
&\quad - l_f F_{df}(t)\cos(\varphi(t)) + l_r F_{dr}(t)\cos(\varphi(t))\\
&\quad + k_s l_s\delta_s(t) + l_s F_{ds}(t) - (h_s + \delta_{tr} + \delta_s(t))R_s\\
0 &= -m_s\ddot{x}_s(t) - k_s\delta_s(t)\cos(\varphi(t)) - F_{ds}(t)\cos(\varphi(t))\\
&\quad - R_s\sin(\varphi(t)) - m_s g\\
0 &= -m_s\ddot{y}_s(t) - k_s\delta_s(t)\sin(\varphi(t)) - F_{ds}(t)\sin(\varphi(t))\\
&\quad + R_s\cos(\varphi(t))\\
0 &= -J_s\ddot{\varphi}(t) + R_s\delta_{tr}
\end{aligned} \tag{4}$$

where

$$y_s(t) = (h_s + \delta_s(t))\sin(\varphi(t)) + l_s(1 - \cos(\varphi(t))) \tag{5}$$

$F_{df}(t), F_{dr}(t)$ and $F_{ds}(t)$ represent the resistance forces produced by the MR dampers d_f, d_r and d_s, respectively.

Considering the fact that the amplitude of the external excitation $w_f(t)$ is small compared to the length of the beam, it can be assumed that $\sin(\varphi(t)) = 0$, $\cos(\varphi(t)) = 1$ in equations (4) and (5), whereas $\sin(\phi(t)) = \phi(t)$ and $\cos(\varphi(t)) = 1$ in equations (1)–(3). Based on these assumptions, equations (1)–(5) can be simplified as follows

$$\begin{aligned}
m_t\ddot{x}_t(t) &= -k_f\delta_f(t) - k_r\delta_r(t) + k_s\delta_s(t) - F_{df} - F_{dr} + F_{ds}\\
J_r\ddot{\varphi}(t) &= -k_f l_f\delta_f(t) + k_r l_r\delta_r(t) - l_f F_{df} + l_r F_{dr}\\
&\quad + k_s l_s\delta_s(t) + l_s F_{ds}\\
m_s\ddot{x}_s(t) &= -k_s\delta_s(t) - F_{ds}(t)
\end{aligned} \tag{6}$$

where

$$\delta_f(t) = x_t(t) + l_f\phi(t) - w_f(t) \tag{7}$$

$$\delta_r(t) = x_t(t) - l_r\phi(t) \tag{8}$$

$$\delta_s(t) = x_s(t) - x_t(t) - l_s\phi(t) \tag{9}$$

$$J_r = J_t + J_s + m_s h_s^2. \tag{10}$$

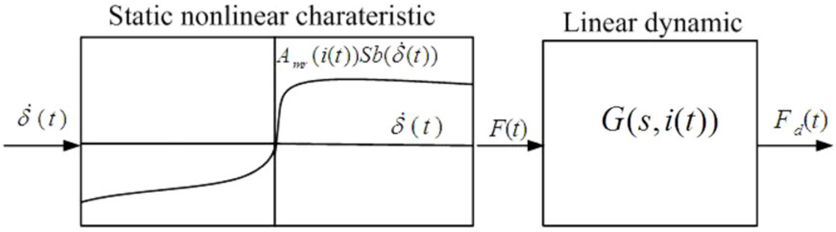

Figure 3. The nonparametric model of MR dampers used in the present study.

Rewriting equations (6) in a matrix form and taking equations equations (7)–(10) into account yield:

$$M\ddot{X}(t) + KX(t) = RW_{\text{in}}(t) \tag{11}$$

where

$$X(t) = (x_{\text{t}}(t), \varphi(t), x_{\text{s}}(t))^{\text{T}}, \tag{12}$$

$$W_{\text{in}}(t) = (F_{df}(t), F_{dr}(t), F_{ds}(t), \dot{w}_{\text{f}}(t))^{\text{T}} \tag{13}$$

$$M = \begin{bmatrix} m_{\text{t}} & 0 & 0 \\ 0 & J_{\text{r}} & 0 \\ 0 & 0 & m_{\text{s}} \end{bmatrix} \tag{14}$$

$$K = \begin{bmatrix} k_{\text{f}} + k_{\text{r}} + k_{\text{s}} & k_{\text{f}}l_{\text{f}} - k_{\text{r}}l_{\text{r}} + k_{\text{s}}l_{\text{s}} & -k_{\text{s}} \\ k_{\text{f}}l_{\text{f}} - k_{\text{r}}l_{\text{r}} + k_{\text{s}}l_{\text{s}} & k_{\text{f}}l_{\text{f}}^2 + k_{\text{r}}l_{\text{r}}^2 + k_{\text{s}}^2l_{\text{s}}^2 & -k_{\text{s}}l_{\text{s}} \\ -k_{\text{s}} & -k_{\text{s}}l_{\text{s}} & k_{\text{s}} \end{bmatrix} \tag{15}$$

$$R = \begin{bmatrix} -1 & -1 & 1 & k_{\text{f}} \\ -l_{\text{f}} & l_{\text{r}} & l_{\text{s}} & k_{\text{f}}l_{\text{f}} \\ 0 & 0 & -1 & 0 \end{bmatrix}. \tag{16}$$

Equation (11) shows that the pitch plane suspension system is a 3dof system whose mass and stiffness matrices are defined by equations (14) and (15), respectively. $W_{\text{in}}(t)$ is an external input vector to the system, which contains a disturbance input $\dot{w}_{\text{f}}(t)$, and the resistance forces $F_{df}(t)$, $F_{dr}(t)$ and $F_{ds}(t)$ from the three MR dampers.

2.2. Nonparametric model of MR dampers

Generally speaking, there are two methods for modelling MR dampers. The first is the parametric modelling technique that represents a MR damper using a series of linear and nonlinear components such as springs and dampers with specific parameters. The stress–strain relationship of the Bingham viscoplastic described by Shames and Cozzarelli [23] is often used to describe the MR damper behaviour. In this model, the plastic viscosity is defined as the slope of measured shear stress versus shear strain rate. In 1996, Spencer *et al* [24] proposed an effective parametric model of MR dampers based on an extension of the Bouc–Wen model, proposed in 1976 by Wen *et al* [25]. However, this model cannot easily be solved numerically due to the stiffness of the equation used to describe MR dampers. The second method is known as the nonparametric modelling technique. This technique usually uses an analytical expression to describe the characteristics of a MR damper based on both experimental data and MR damper physics. Hsu and Meyer [26] and McClamroch and Gavin [27] used trigonometric functions to describe the MR damper characteristics. However their model cannot capture the saturation of MR dampers' resistance force. Recently, Song *et al* [22] proposed a simple nonparametric model where the characteristics of a commercial MR damper are represented by a series of continuous functions and differential equations, which can be easily solved using numerical simulation techniques. This nonparametric model is as shown in figure 3 and is used, in this study, to represent the dynamics of the MR dampers.

In figure 3, $\dot{\delta}(t)$ is the relative velocity across an MR damper. $Sb(\dot{\delta}(t))$ represents the static nonlinear characteristic of the MR damper. The amplitude of the static characteristic is a function of the MR damper current $i(t)$ which is represented by $A_{\text{mr}}(i(t))$. $F(t)$ is the output of the static nonlinear characteristic. $G(s, i(t))$ is the transfer function of a linear dynamic whose characteristic parameters also change with the value of the control current $_i(t)$.

It can be clearly seen from figure 3 that the MR damper model consists of a nonlinear static characteristic followed by a linear dynamic. The linear dynamic represents the hysteresis loop associated with MR damper physics, and the nonlinear characteristic represents the MR damper nonlinearity.

To represent the nonlinear characteristic, Song *et al* [22] used the following equations:

$$F(t) = A_{\text{mr}}(i(t))Sb(\dot{\delta}(t)) \tag{17}$$

where

$$A_{\text{mr}}(i(t)) = \sum_{j=0}^{r} A_j i^j(t) \tag{18}$$

is a polynomial function of the MR damper control current $i(t)$, and $Sb(\dot{\delta}(t))$ is a function of the form:

$$\begin{aligned} Sb(\dot{\delta}(t)) = {} & [(b_0 + b_1|\dot{\delta}(t) - V_0|)^{b_2(\dot{\delta}(t)-V_0)} \\ & - (b_0 + b_1|\dot{\delta}(t) - V_0|)^{-b_2(\dot{\delta}(t)-V_0)}] \\ & \times [b_0^{b_2(\dot{\delta}(t)-V_0)} + b_0^{-b_2(\dot{\delta}(t)-V_0)}]^{-1} \end{aligned} \tag{19}$$

where $b_0 > 1$, $b_1 > 0$, $b_2 > 0$ and V_0 are all constants.

To describe the linear dynamics $G(s, i(t))$, Song *et al* [22] used a first order linear system as described by:

$$\dot{z}(t) = -(e_0 + e_1 i(t) + e_2 i^2(t))z(t) + e_3 F(t) \tag{20}$$

$$F_d(t) = (e_0 + e_1 i(t) + e_2 i^2(t))z(t) + e_4 F(t) \tag{21}$$

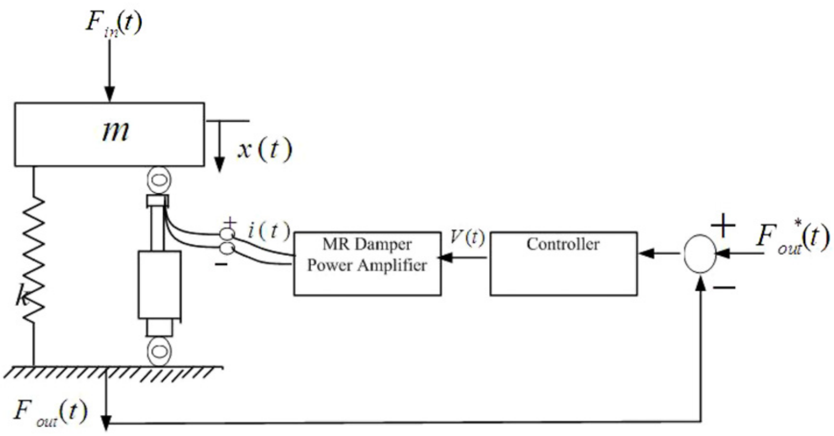

Figure 4. An illustration of conventional MR damper based vibration control.

Table 1. The estimated characteristic parameters of a commercial MR damper.

Parameter	Value	Parameter	Value	Parameter	Value
A_0	164.8	e_0	299.7733	b_0	5.8646
A_1	1316.5	e_1	−210.320	b_1	0.006
A_2	1407.8	e_2	566.0	b_2	0.2536
A_3	−1562.8	e_3	1	V_0	0.6248
A_4	388.8	e_4	0		

where $e_j, j = 0, \ldots, 4$ are constants determined by the damper characteristics.

Song *et al* [22] also showed that, using a mean square error based optimization approach, the values of parameters in equations (17)–(21) of a commercial MR damper can be determined. Table 1 shows the parameter estimation results Song *et al* [22] have obtained for a commercial MR damper.

In this case, $G(s, i(t))$ can be obtained from equations (20) and (21) as:

$$G(s, i(t)) = \frac{e_0 + e_1 i(t) + e_2 i(t)^2}{(s + e_0 + e_1 i(t) + e_2 i(t)^2)} \tag{22}$$

$$A_{mr}(i(t)) = \sum_{j=0}^{4} A_j i^j(t) = (A_0 + A_1 i(t) + A_2 i^2(t) + A_3 i^3(t) + A_4 i^4(t)) \tag{23}$$

and the nonparametric model of the MR damper, which represents a dynamic relationship between the MR damper damping force and the control current, can be simplified as:

$$\dot{F}_d(t) + e_0 F_d(t)\left(1 + \frac{e_1}{e_0} i(t) + \frac{e_2}{e_0} i^2(t)\right) = A_0 e_0 S b(\dot{\delta}(t))\left(1 + \frac{e_1}{e_0} i(t) + \frac{e_2}{e_0} i^2(t)\right) \times \left(1 + \frac{A_1}{A_0} i(t) + \frac{A_2}{A_0} i^2(t) + \frac{A_3}{A_0} i^3(t) + \frac{A_4}{A_0} i^4(t)\right). \tag{24}$$

In this study, equation (24) will be used to describe the dynamics of the three MR dampers, d_f, d_s, and d_r. The resistance force and control current of the three MR dampers will be denoted by $F_{df}(t) i_f(t)$, $F_{ds}(t) i_s(t)$, and $F_{dr}(t) i_r(t)$, respectively.

3. MR damper based implementation of nonlinear damping for vibration control of the pitch plane suspension system

For most currently available MR damper based vibration control systems, MR dampers are used as actuators in a feedback control loop to produce a resistance force to achieve a desired vibrating system response. Figure 4 shows an illustration of how this widely adopted approach is used to suppress the transmission of vibration from a source on the top to the supporting base of a single degree of freedom structural system. In figure 4, $F_{in}(t)$ and $F_{out}(t)$ represent the vibration input, and the system response: the net force from both the spring and damper, respectively. $x(t)$ is the displacement of mass m. k represents the stiffness of the spring. $i(t)$, $V(t)$, and $F^*_{out}(t)$ are the MR damper control current, MR damper power amplifier input voltage, and the desired system force response, respectively.

However, in the present study, the use of the MR dampers follows a new approach which is totally different from the conventional MR damper based vibration control in figure 4. This approach is to use an MR damper as a viscous damper rather than an actuator in a feedback control loop.

First, fixed control currents i_{f0} and i_{r0} are applied to MR dampers d_f and d_r, respectively. Consequently, according to the MR damper model equation (24), the resistance forces $F_{df}(t)$ and $F_{dr}(t)$ of the MR dampers can be obtained from the solution to the differential equations

$$\dot{F}_{df}(t) + e_0 F_{df}(t)\left(1 + \frac{e_1}{e_0} i_{f0} + \frac{e_2}{e_0} i_{f0}^2\right) = A_0 e_0 S b(\dot{\delta}_f(t))\left(1 + \frac{e_1}{e_0} i_{f0} + \frac{e_2}{e_0} i_{f0}^2\right) \times \left(1 + \frac{A_1}{A_0} i_{f0} + \frac{A_2}{A_0} i_{f0}^2 + \frac{A_3}{A_0} i_{f0}^3 + \frac{A_4}{A_0} i_{f0}^4\right) \tag{25}$$

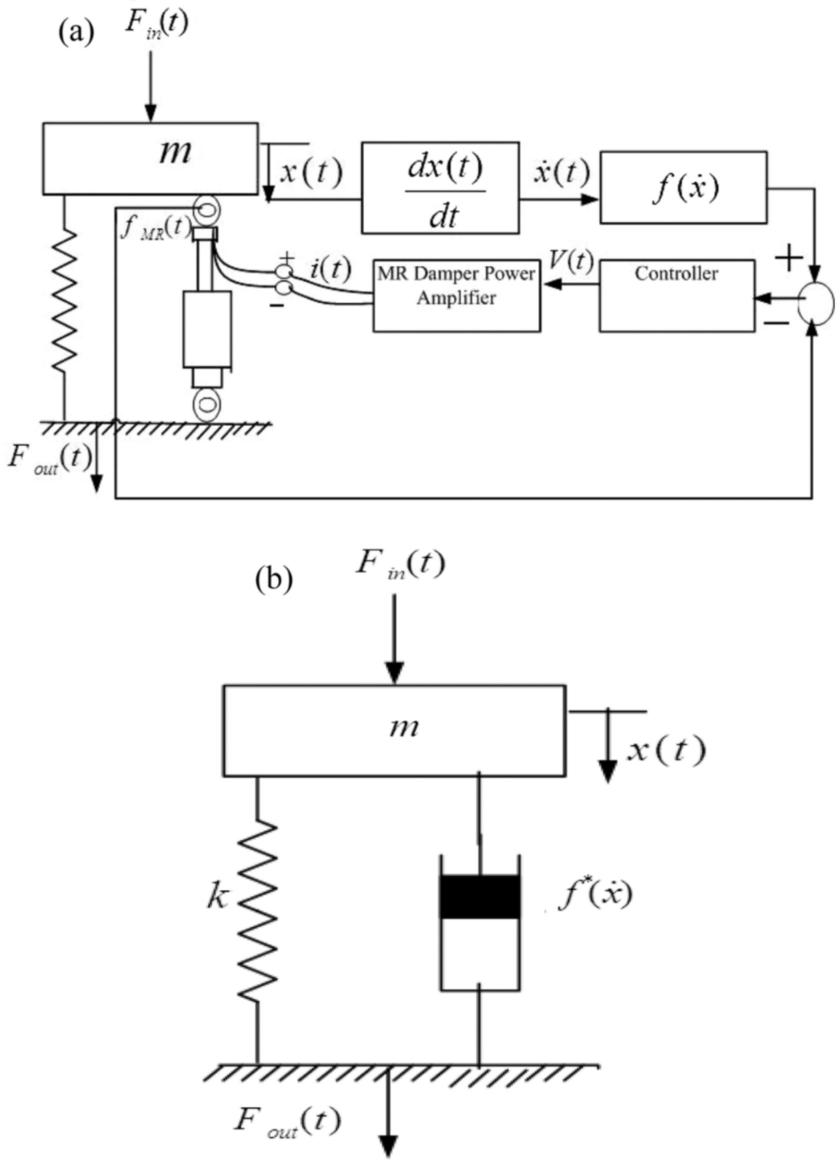

Figure 5. An illustration of the new MR damper based vibration control. (a) The system configuration for the case of a sdof system. (b) The equivalent structural system.

and

$$\dot{F}_{dr}(t) + e_0 F_{dr}(t)\left(1 + \frac{e_1}{e_0} i_{r0} + \frac{e_2}{e_0} i_{r0}^2\right)$$
$$= A_0 e_0 S b(\dot{\delta}_r(t))\left(1 + \frac{e_1}{e_0} i_{r0} + \frac{e_2}{e_0} i_{r0}^2\right)$$
$$\times \left(1 + \frac{A_1}{A_0} i_{r0} + \frac{A_2}{A_0} i_{r0}^2 + \frac{A_3}{A_0} i_{r0}^3 + \frac{A_4}{A_0} i_{r0}^4\right) \qquad (26)$$

respectively.

Secondly, a feedback control is introduced for the resistance force of the MR damper d_s to achieve the desired nonlinear damping characteristic. This is a new MR damper based vibration control method. Figure 5(a) shows an illustration of how this new method can be used to address the same vibration control problem in figure 4. Figure 5(b) shows a vibrating system which is equivalent to the system in figure 5(a) where $f_{MR}(t)$ is the MR damper resistance force and f^* is a desired damping characteristic to be implemented. Clearly, as illustrated in figure 5(b), the objective of the new control is to make the MR damper behave like a viscous damper with a desired damping characteristic $f^*(\dot{x}(t))$. The new method combines the feedback control with MR damper physics so that a guaranteed stability and robustness for the overall system can be readily achieved together with a desired performance.

In this study, the new method is used in the multi-degree of freedom pitch plane suspension system described in section 2.1 and applied to an MR damper d_s to implement a cubic nonlinear damping characteristic. That is, to control the MR damper resistance force to make the force approach to the reference

$$F_{ds}^*(t) = a_s \dot{\delta}_s^3(t). \qquad (27)$$

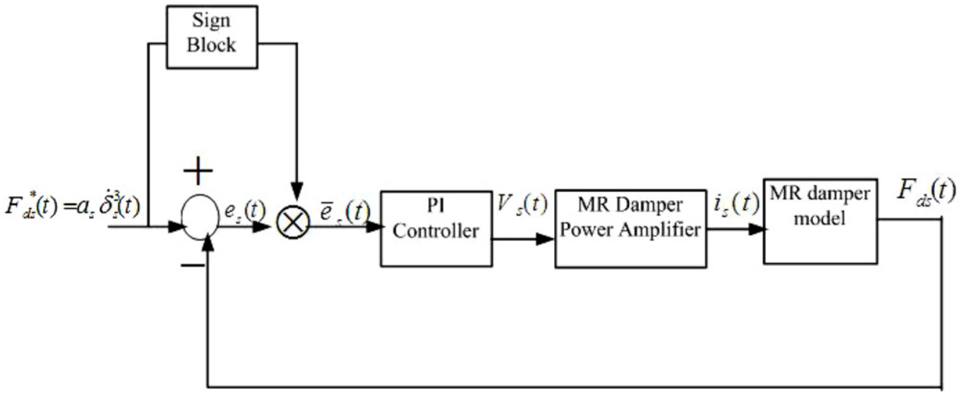

Figure 6. The feedback control system for MR damper d_s.

The objective is to exploit the beneficial effects of nonlinear damping, which have been revealed in previous studies [9–11], to conduct an effective semi-active vibration control for the system. This is, as far as we are aware, a totally new solution to the pitch plane suspension system vibration control problem. For this purpose, the feedback control system as shown in figure 6 is applied to control the resistance force of the MR damper d_s. From figure 6, it is known that the control current $i_s(t)$ for the MR damper d_s is determined by a PI control law as follows:

$$i_s(t) = K_c[K_P\bar{e}_s(t) + K_I\int_0^t \bar{e}_s(t)\,dt] \tag{28}$$

where K_c is the gain of the MR damper control circuit, K_p and K_I are the proportional and integration gains of the PI controller,

$$\bar{e}_s(t) = \mathrm{sgn}(F^*_{ds}(t))e_s(t) \tag{29}$$

$$e_s t = F^*_{ds}(t) - F_{ds}(t) \tag{30}$$

where $F_{ds}(t)$ is the resistance force of the MR damper d_s which can be described using the MR damper model equation (24) as

$$\dot{F}_{ds}(t) + e_0F_{ds}(t)\left(1 + \frac{e_1}{e_0}i_s(t) + \frac{e_2}{e_0}i_s^2(t)\right)$$
$$= A_0e_0Sb(\dot{\delta}_s(t))\left(1 + \frac{e_1}{e_0}i_s(t) + \frac{e_2}{e_0}i_s^2(t)\right)$$
$$\times\left(1 + \frac{A_1}{A_0}i_s(t) + \frac{A_2}{A_0}i_s^2(t) + \frac{A_3}{A_0}i_s^3(t) + \frac{A_4}{A_0}i_s^4(t)\right). \tag{31}$$

Equations (27)–(31) provide a comprehensive description of the resistance force of MR damper d_s.

It is worth pointing out that the PI control law for the control current of MR damper d_s described by equations (28)–(30) is different from a standard PI controller in that a sign function of the reference input has to be applied to the error signal before a standard PI control law can be applied. This is because of the physical relationship between the MR damper resistance force and control current. A more detailed explanation of the necessity of introducing this sign function is provided in the appendix.

Considering the dynamic behaviours of MR dampers d_f, d_r, and d_s, described by equations (25), (26) and (27)–(31), it is known that under the above described new approach to the MR damper based vibration control, in the steady state of the pitch plane suspension system,

$$F_{ds}(t) \approx a_s\dot{\delta}^3(t) \tag{32}$$

$$F_{df}(t) \approx a_f\dot{\delta}_f(t) \tag{33}$$

$$F_{dr}(t) \approx a_r\dot{\delta}_r(t) \tag{34}$$

where a_f and a_r are the equivalent linear damping characteristic parameters achieved by applying a fixed control current to MR dampers d_f and d_r, respectively. Note that equations (33) and (34) are a considerably simplified representation of MR dampers d_f and d_r. The simplification is made to relate the currently studied pitch plane suspension system to the nonlinearly damped mdof systems that have been investigated in [11].

For this purpose, substituting equations (32)–(34) into

$$W_{in}(t) = (F_{df}(t), F_{dr}(t), F_{ds}(t), \dot{w}_f(t))^T$$

for $F_{ds}(t), F_{df}(t), F_{dr}(t)$, respectively, in equation (11) yields, after some manipulations, an overall description for the pitch plane suspension system as

$$M\ddot{X}(t) + C\dot{X}(t) + KX(t) + Da_s\dot{\delta}_s^3(t) = R_UU(t) \tag{35}$$

where

$$U(t) = (w_f(t), \dot{w}_f(t), \ddot{w}_f(t))^T \tag{36}$$

$$C = \begin{bmatrix} a_f + a_r & a_fl_f - a_rl_r & 0 \\ a_fl_f - a_rl_r & a_fl_f^2 + a_rl_r^2 & 0 \\ 0 & 0 & 0 \end{bmatrix} \tag{37}$$

$$D = [\,-1 \;\; -l_s \;\; 1]^T \tag{38}$$

$$R_U = \begin{bmatrix} k_f & a_f & 0 \\ k_fl_f & a_fl_f & 0 \\ 0 & 0 & 0 \end{bmatrix}. \tag{39}$$

Clearly, in this case, the pitch suspension system can be approximated by a 3dof system with a cubic nonlinear damping characteristic. Therefore, it is expected

Table 2. The mass and geometrical parameters of the pitch suspension system used in the simulation studies.

Parameter	Designation	Value
Distance (P_g, P_f)	l_f	0.700 m
Distance (P_g, P_r)	l_r	0.700 m
Distance (P_g, P_s)	l_s	0.525 m
Mean distance (P_{gs}, P_s)	h_s	0.430 m
Length of the beam	L	1.500 m
Height of the beam	a	0.044 m
Width of the beam	b	0.147 m
Mass of the beam (including masses of the elements permanently connected with the beam)	m_t	102.13 kg
Moment of inertia of the beam (including the elements permanently connected with the beam) with regard to its pitch axis passing through P_g	J_t	19.14 kg m^{-2}
Front (rear) suspension-set spring stiffness	k_f (k_r)	35 861 N m^{-1}
Mass of the body suspended above the beam	m_s	35.09 kg
Moment of inertia of the body with regard to its pitch axis passing through P_{gs}	J_s	0.23 kg m^{-2}
Body suspension-set spring stiffness	k_s	14 434 N m^{-1}

that the beneficial effects of nonlinear viscous damping on vibration suppression that have been revealed in the previous studies [9–11] would be achieved by the MR damper based implementation of nonlinear damping in the system.

4. Simulation studies

In this section, the effectiveness of the MR damper based implementation of nonlinear damping and the benefits of this new approach for the pitch plane suspension system vibration control are demonstrated by numerical simulation studies. In the studies, equation (11) is used to generate the dynamic response of the pitch plane suspension system. The resistance forces $F_{df}(t)$, $F_{dr}(t)$, and $F_{ds}(t)$ of MR dampers d_f, d_r and d_s are determined by equations (25), (26) and (28)–(31), respectively. The mass and geometrical parameters of the pitch suspension system used for the studies are listed in table 2.

4.1. The effectiveness of the MR damper based implementation of nonlinear damping

In order to demonstrate the effectiveness of using the feedback control shown in figure 6 to achieve a desired nonlinear damping characteristic, a sinusoidal displacement excitation $w_f(t)$ with amplitude 70 mm is applied to the pitch plane suspension system model equation (11). The desired nonlinear damping characteristic for MR damper d_s is defined by equation (27) with $a_s = 220$ N (s m^{-1})^3, that is,

$$F^*_{ds}(t) = 220\dot{\delta}^3_s(t). \tag{40}$$

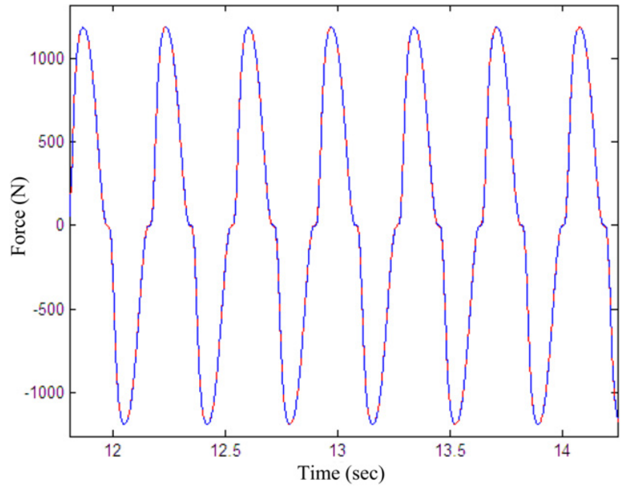

Figure 7. A comparison between the desired and actual resistance forces of MR damper d_s when the pitch plane suspension system is excited by a 2.5 Hz sinusoidal input. Solid (red): actual force; dashed (blue): desired force.

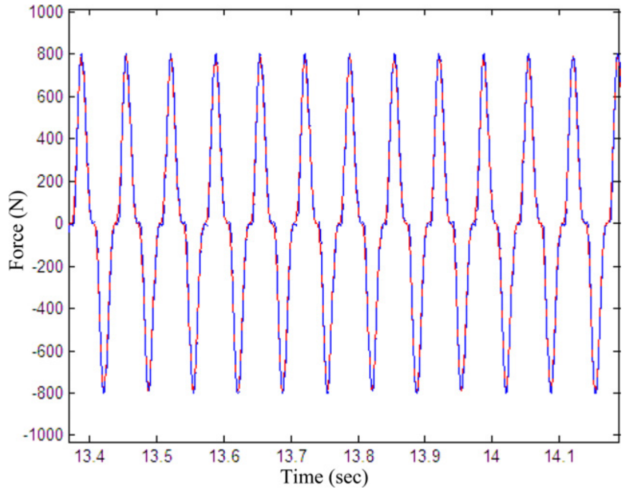

Figure 8. A comparison between the desired and actual resistance forces of MR damper d_s when the pitch plane suspension system is excited at a 15 Hz sinusoidal input. Solid (red): actual force; dashed (blue): desired force.

Two cases were investigated by simulating the pitch plane suspension system where the driving frequencies of the sinusoidal excitation $w_f(t)$ are 2.5 Hz and 15 Hz, respectively. For MR dampers d_f and d_r, the control current was fixed at $i_{r0} = i_{f0} = 0.25$ A. The PI controller parameters in the control system for MR damper d_s were determined as $K_P = 1.3 \times 10^{-3}$ and $K_I = 2$ in this study. Figures 7 and 8 show a comparison between the desired and actual resistance force of MR damper d_s in the 2.5 Hz and 15 Hz external excitation cases, respectively.

It can be observed from figures 7 and 8 that the actual forces track the desired results very well in the two different driving frequency cases. On the other hand, figures 9 and 10 show that the MR damper control current in the two excitation cases is all in the range of [−0.3 A, 0.3 A], which is within the normal operating range of [−2 A, 2 A] of

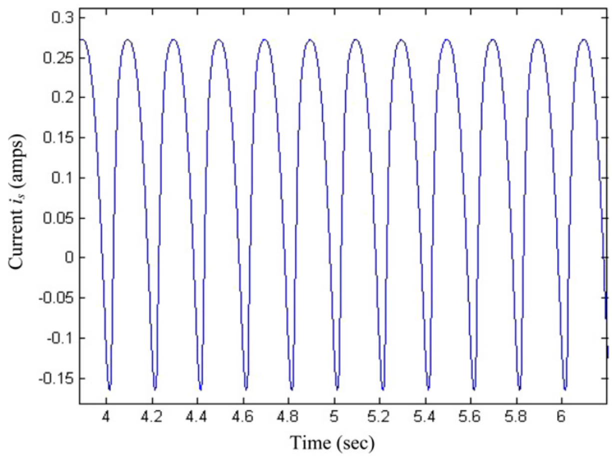

Figure 9. Current i_s supplied to MR damper d_s when the pitch plane suspension system is excited by a 2.5 Hz sinusoidal input.

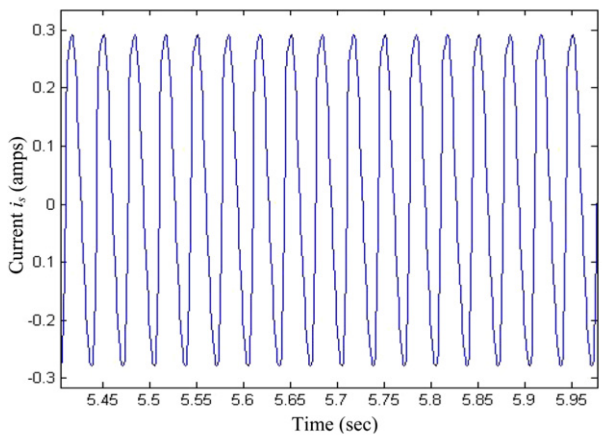

Figure 10. Current i_s supplied to MR damper d_s when the pitch plane suspension system is excited by a 15 Hz sinusoidal input.

MR damper currents. These results clearly demonstrate the effectiveness of the MR damper based implementation of nonlinear damping.

4.2. The beneficial effects of nonlinear damping on the pitch plane suspension system vibration control

As has been mentioned above, in the pitch plane suspension system considered in this study, MR dampers d_f and d_r are used to approximately implement two linear dampers and MR damper d_s is used to implement a cubic nonlinear damping characteristic. The main objective of the simulation studies is to demonstrate the beneficial effects of a cubic nonlinear damping implemented by using MR damper d_s on the pitch plane suspension system vibration control.

For this purpose, a sinusoidal displacement excitation $w_f(t)$ with amplitude 70 mm was applied to the pitch plane suspension system model equation (11) to generate the acceleration response $\ddot{x}_s(t)$ of the passenger seat/cabin to the sinusoidal input at each of the following discrete frequencies

2, 2.5, 3, 4, 4.6, 5, 6, 6.28, 7, 8, 9, 10, 11, 12,
13, 14, 15, 16, 17, 18, 19, 20, 21, 22, 23, 24 Hz.

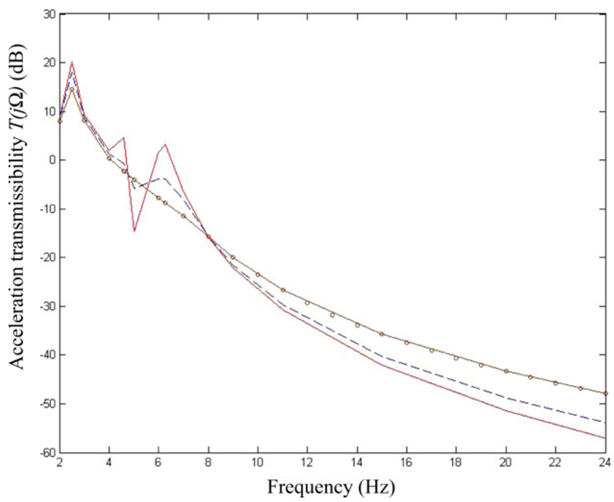

Figure 11. Acceleration transmissibility of the pitch plane suspension system under three different fittings of MR dampers. Solid (red): MR damper fitting (a); dashed (blue): MR damper fitting (b); circle (brown): MR damper fitting (c).

From the system responses and corresponding input excitations, the acceleration transmissibility as defined by

$$T(\mathrm{j}\Omega) = \left| \frac{(\mathrm{j}\Omega)^2 X_s(\mathrm{j}\Omega)}{(\mathrm{j}\Omega)^2 W_f(\mathrm{j}\Omega)} \right| = \left| \frac{X_s(\mathrm{j}\Omega)}{W_f(\mathrm{j}\Omega)} \right| \tag{41}$$

and the acceleration RMS transmissibility as defined by

$$T_{\mathrm{RMS}}(\Omega) = \frac{\sqrt{\int_0^{t_{\mathrm{fin}}} [(\ddot{x}_s(t,\Omega))]^2 \,\mathrm{d}t}}{\sqrt{\int_0^{t_{\mathrm{fin}}} [(\ddot{w}_f(t,\Omega))]^2 \,\mathrm{d}t}} \tag{42}$$

can be evaluated. In equations (41) and (42), $X_s(\mathrm{j}\Omega)$ and $W_f(\mathrm{j}\Omega)$ are the Fourier spectra of $x_s(t)$ and $w_f(t)$ at frequency Ω, respectively; t_{fin} denotes the total simulation time; and $\ddot{x}_s(t,\Omega)$ and $\ddot{w}_f(t,\Omega)$ represent the time history of $\ddot{x}_s(t)$ and $\ddot{w}_f(t)$ in the case when $w_f(t)$ is a sinusoidal excitation with frequency Ω.

In the simulation studies, $T(\mathrm{j}\Omega)$ was first evaluated over the above range of discrete frequencies under the following three different fittings of MR dampers in the system:

(a) only MR damper d_s is fitted in the system, but its control current is set to $i_s(t) = 0$.
(b) MR dampers d_f, d_r, and d_s are all fitted in the system, but the control currents for the three MR dampers are all set to zero, that is, $i_f(t) = i_r(t) = i_s(t) = 0$.
(c) MR dampers d_f, d_r, and d_s are all fitted in the system, the control currents for the MR dampers d_f and d_r are set to $i_f(t) = i_r(t) = 0.25$ A but the control current for MR damper d_s is set to $i_s = 0$. The results are shown in figure 11, which show the system's vibration isolation performance in three different cases where MR damper d_s has not been used to implement a desired linear or nonlinear damping characteristic. From the results, it can be found that, under MR damper fitting (a), the pitch plane suspension system behaves like a typical 3dof system with its frequency response having three resonant peaks

at frequencies 2.5 Hz, 4.6 Hz and 6.28 Hz, respectively. However, under MR damper fitting (b) where, compared with MR damper fitting (a), two more MR dampers are fitted into the system, the resonant peaks are reduced by the inherent damping effects of the MR dampers, although zero control current is applied to the MR dampers. Moreover, it can be observed that under MR damper fitting (c) where a fixed control current is applied to MR dampers d_f and d_r, a more significant damping effect is produced such that the second and third resonant peaks of the system become almost invisible.

Secondly, a desired cubic nonlinear damping and its equivalent linear damping were implemented by MR damper d_s, using the damping force feedback control system in figure 6 to demonstrate the beneficial effects of nonlinear damping on the system vibration control. By equivalent linear damping, we mean that the linear damping can achieve the same reduction of the first resonant peak as can be achieved by a desired cubic nonlinear damping. Two cases were investigated which are:

(d) only MR damper d_s is fitted in the system to implement a desired cubic nonlinear damping and its equivalent linear damping, respectively.

(e) MR damper d_s is used to implement a desired cubic nonlinear damping and its equivalent linear damping, respectively, and MR dampers d_f, and d_r are fitted in the system with control currents set to be $i_f(t) = i_r(t) = 0.25$ A.

In both cases, the MR damping force controller parameters are the same as used in section 4.1.

In case (d), the desired nonlinear and its equivalent linear damping characteristics were specified to be

$$F^*_{ds}(t) = 1100\dot{\delta}_s^3(t) \tag{43}$$

and

$$F^*_{ds}(t) = 1150\dot{\delta}_s, \tag{44}$$

respectively. The two damping characteristics are equivalent in the sense that they can both reduce the first resonant peak of the system to about the same level. Figure 12 shows a comparison of the system acceleration transmissibility under the following three situations in case (d):

- no desired damping is implemented by MR damper d_s (i_s=0);
- desired nonlinear damping (43) is implemented by d_s; and
- equivalent linear damping (44) is implemented by d_s.

From the comparison, the advantage of the desired nonlinear damping equation (43) over the equivalent linear damping equation (44) can be clearly observed. Basically, compared with the case of introduction of an equivalent linear damping, a significantly reduced acceleration transmissibility can be achieved over the isolation frequency range by the desired nonlinear damping.

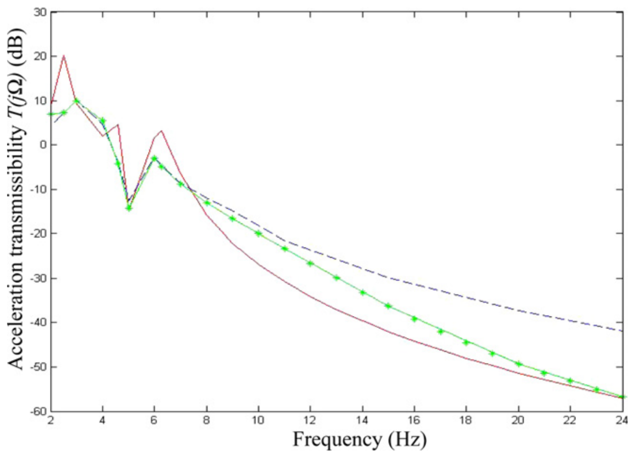

Figure 12. Comparison of the system acceleration transmissibility in case (d). Red solid: no implementation of desired damping by MR damper d_s; green crossed: implementation of desired nonlinear damping (43) by d_s; blue dashed: implementation of equivalent linear damping (44) by d_s.

In case (e), the desired nonlinear and its equivalent linear damping characteristics are first specified to be

$$F^*_{ds}(t) = 160\dot{\delta}_s^3(t) \tag{45}$$

and

$$F^*_{ds}(t) = 460\dot{\delta}_s^3(t), \tag{46}$$

respectively. The comparison of the system acceleration transmissibility under the following three situations:

- no desired damping is implemented by MR damper d_s ($i_s = 0$);
- desired nonlinear damping (45) is implemented by d_s; and
- equivalent linear damping (46) is implemented by d_s.

was made; the results are shown in figure 13.

Then, the desired nonlinear and its equivalent linear damping characteristics are specified to be

$$F^*_{ds}(t) = 220\dot{\delta}_s^3(t) \tag{47}$$

and

$$F^*_{ds}(t) = 526\dot{\delta}_s^3(t), \tag{48}$$

respectively, to compare the system acceleration transmissibility under the following three situations:

- no desired damping is implemented by MR damper d_s ($i_s = 0$);
- desired nonlinear damping (47) is implemented by d_s; and
- equivalent linear damping (48) is implemented by d_s.

The results are shown in figure 14.

From the results in figures 13 and 14, the same beneficial effects of nonlinear damping on the system vibration isolation as shown in figure 12 can be clearly observed. That is, although a similar vibration control level can be reached over the resonant frequency range by both a desired cubic nonlinear

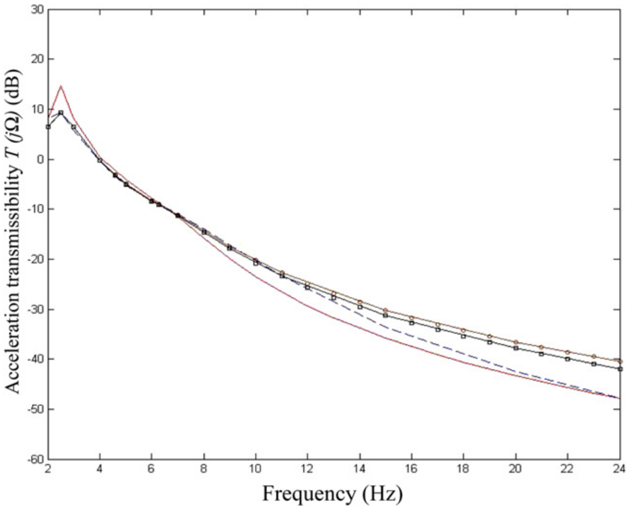

Figure 13. Comparison of the system acceleration transmissibility in case (e) under the first choice of the desired nonlinear and its equivalent linear damping characteristics. Red solid: no implementation of desired damping by MR damper d_s; blue dashed: implementation of desired nonlinear damping (45) by d_s; brown circle: implementation of equivalent linear damping (46) by d_s. Black square: implementation of an equivalent on/off skyhook control where $i_e = 0.2$ A.

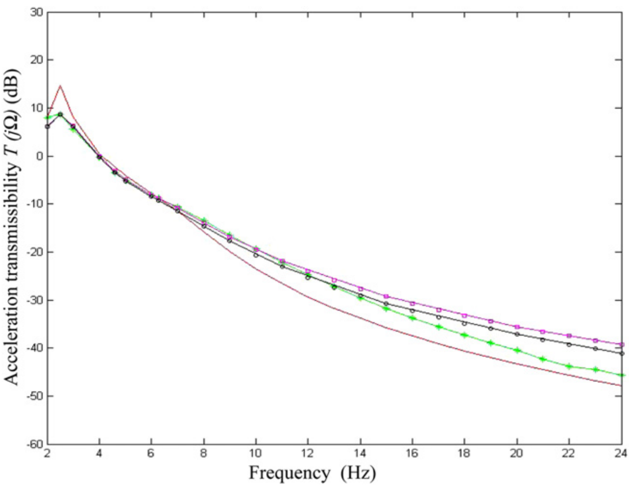

Figure 14. Comparison of the system acceleration transmissibility in case (e) under the second choice of the desired nonlinear and its equivalent linear damping characteristics. Red solid: no implementation of desired damping by MR damper d_s; green star: implementation of desired cubic nonlinear damping (47) by d_s; pink square: implementation of equivalent linear damping (48) by d_s. black circle: implementation of an equivalent on/off skyhook control where $i_e = 0.24$ A.

damping and its equivalent linear damping, much better vibration isolation can be obtained by the nonlinear damping over isolation frequency ranges. In addition, a comparison of the results in figures 13 and 14 indicates that although the increase of nonlinear damping or its equivalent linear damping can all improve the system vibration control performance over the resonant frequency region, nonlinear damping can always achieve a better overall vibration control performance. This is because over isolation frequency ranges the system

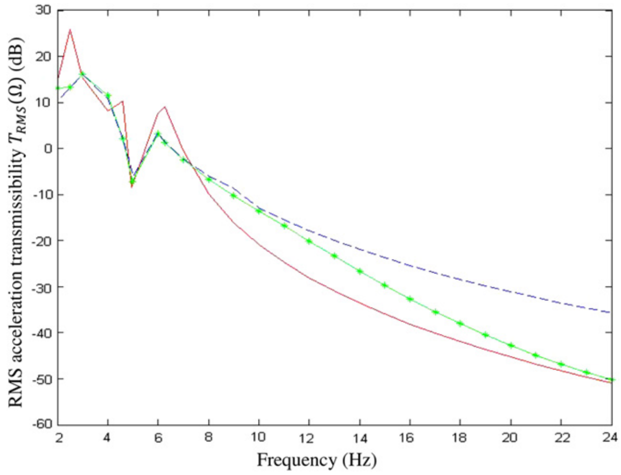

Figure 15. Comparison of the system RMS acceleration transmissibility in case (d). Red solid: no implementation of desired damping by MR damper d_s; green crossed: implementation of desired nonlinear damping (43) by d_s; blue dashed: implementation of equivalent linear damping (44) by d_s.

acceleration transmissibility under nonlinear damping is always less than the transmissibility under linear damping.

The conclusions reached from analysis of the results in figures 12–14 are all consistent with the theoretical analyses in the previous studies for both single and multi-degree of freedom systems. Therefore, the beneficial effects of nonlinear damping on the vibration control of the pitch plane suspension system has been demonstrated by the above simulation studies.

It is worth pointing out that the acceleration transmissibility used to evaluate the performance of the pitch plane suspension as shown in figures 12–14 is, rigorously speaking, a concept of linear systems where a sinusoidal input at a frequency will produce a sinusoidal output at the same frequency. However, the introduction of nonlinear damping and the inherent nonlinear property of MR dampers imply that the response of the pitch plane suspension system to a single frequency sinusoidal input may contain more than one frequency component. Considering this, the acceleration RMS transmissibility (42) was also evaluated for each of the cases analysed above. The objective is to perform a more comprehensive analysis to confirm the conclusions that have been reached above using the acceleration transmissibility concept. The acceleration RMS transmissibility concept takes the system response to a sinusoidal input over all possible output frequencies into account so as to be able to accommodate the possible impacts of harmonics etc on the analysis results.

The acceleration RMS transmissibility analysis results are shown in figures 15–17, which correspond to the acceleration transmissibility results in figures 12–14. From the acceleration RMS transmissibility analyses, it is obvious that the same conclusions regarding the beneficial effects of nonlinear damping on the system vibration control can be reached. The similarity between the acceleration transmissibility and its corresponding acceleration RMS

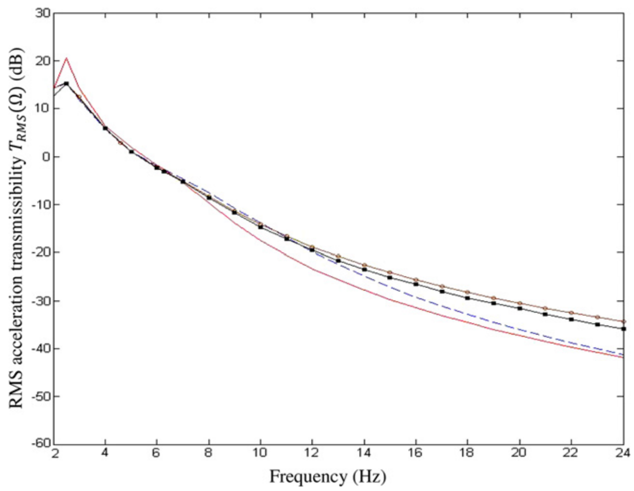

Figure 16. Comparison of the system RMS acceleration transmissibility in case (e) under the first choice of the desired nonlinear and its equivalent linear damping characteristics. Red solid: no implementation of desired damping by MR damper d_s; blue dashed: implementation of desired nonlinear damping (45) by d_s; brown star: implementation of equivalent linear damping (46) by d_s; black square: implementation of an equivalent on/off skyhook control with $i_e = 0.2$ A.

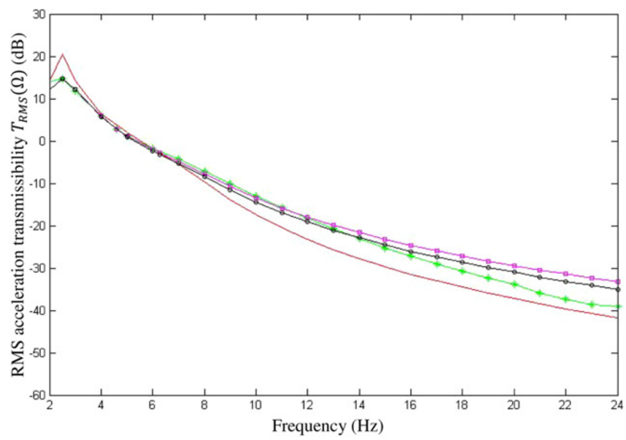

Figure 17. Comparison of the system RMS acceleration transmissibility in case (e) under the second choice of the desired nonlinear and its equivalent linear damping characteristics. Red solid: no implementation of desired damping by MR damper d_s; green star: implementation of desired nonlinear damping (47) by d_s; pink square: implementation of equivalent linear damping (48) by d_s; black circle: implementation of an equivalent on/off skyhook control with $i_e = 0.24$ A.

transmissibility indicates that the harmonics in the system response that can be induced by system nonlinearities basically have no significant effect on the vibration isolation performance of the pitch plane suspension system.

Many MR damper based control methods are available for vehicle suspension systems. Among these, the on/off skyhook control is one of the most widely used techniques (Cebon *et al* [28], Simon and Ahmadian [29]). In order to compare the performances of the new nonlinear damping approach and the on/off skyhook control, the on/off skyhook control was applied to the pitch plane control system in all the cases of simulation studies considered above, where the MR damper control current was determined as follows

$$i_s = \begin{cases} i_e & \text{if } \dot{x}_s(\dot{x}_s - \dot{x}_f) \geq 0 \\ 0 & \text{if } \dot{x}_s(\dot{x}_s - \dot{x}) < 0 \end{cases}$$

Here i_e is the MR damper current, which on/off skyhook control uses to achieve the same vibration suppression as can be achieved by an equivalent linear damper at the first resonance frequency. The results are also shown in figures 13, 14, 16, and 17. From all the results in figures 13, 14 and 16, 17, it can be clearly observed that, although the on/off skyhook control performs better than the equivalent linear viscous damping over the isolation frequency range, the performance of the on/off skyhook control is much worse than that which can be achieved by an equivalent nonlinear damping over the same frequency range. This demonstrates that the nonlinear damping provides better vibration isolation performances for the pitch plane suspension system. It should be noted that if $i_s > i_e$ is used when $\dot{x}_s(\dot{x}_s - \dot{x}_f) \geq 0$ in the on/off skyhook control, then compared to the case of $i_s = i_e$, the system performance will become better over a resonant frequency range but worse over an isolation frequency range.

It should also be emphasized that in the above simulation studies, all the desired nonlinear damping characteristics were not directly used in the system but implemented using MR damper d_s and an associated feedback control system as shown in figure 6. Consequently, it is the effectiveness of this MR damper based implementation of nonlinear damping that ensures that the beneficial effects of nonlinear damping on the vibration control of the pitch plane suspension system can literally be realized.

Finally it is worth mentioning that although only sinusoidal excitations are considered in the present study, the nonlinear damping approach can also achieve better vibration control performance in more general loading conditions. The idea is to use a new concept called output frequency response function (OFRF) (Lang *et al* [30]) to design the nonlinear damping under the considered loading conditions to achieve a required performance. More details can be found in a recent study by Guo and Lang [31].

5. Conclusions

In previous studies, the authors have theoretically proved that the introduction of a cubic nonlinear viscous damping into single and multi-degree of freedom systems can produce the ideal vibration isolation such that the system force transmissibility over resonant frequency regions is modified, but the transmissibility over the isolation frequency regions remains unaffected. In the present study, this beneficial effect of cubic nonlinear viscous damping has been exploited to provide a novel solution to the vibration control of a pitch suspension system. An MR damper has been fitted under the seat/cabin of the pitch plane suspension system; A feedback control is applied to shape the MR damper force/velocity characteristic as a cubic function to implement the desired cubic nonlinear damping characteristic. In contrast

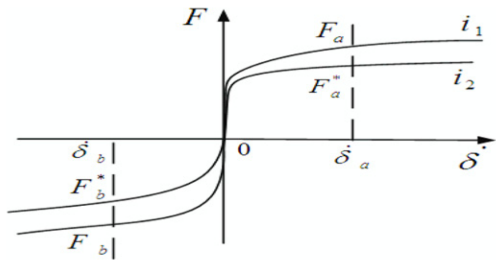

Figure A.1. An illustration of why a sign block is needed for the MR damper PI controller.

to the conventional way of using MR dampers, this study uses MR dampers as dampers rather than actuators in a feedback control loop. Simulation studies have been conducted. The results demonstrate both the effectiveness of the MR damper based implementation of nonlinear damping, and the beneficial effects of nonlinear damping on the pitch plane suspension system vibration control. Based on these, experimental studies on the pitch plane suspension system will be conducted and the results will be reported in a future publication. In the experimental studies, the same setup of an experimental pitch plane suspension system as described in Sapinski and Rosol [32] will be used, and the new nonlinear damping approach will be applied to demonstrate its performance under different experimental conditions.

Acknowledgments

The authors gratefully acknowledge the support of the Royal Society and Engineering and Physical Science Research Council, UK for this work.

Appendix. An explanation of why a sign block is needed for the MR damper PI controller

In order to explain why a sign block is needed for the MR damper PI controller as shown in figure 6, consider two scenarios, which are illustrated figure A.1.

In scenario 1, the relative velocity across MR damper d_s is $\dot{\delta}_a > 0$. The difference between the desired and actual MR damper resistance forces, i.e. control error $e(t) = F_a^* - F_a < 0$. In this case, the output of the sign block is 1, $\bar{e}(t) = e(t) = F_a^* - F_a < 0$. Consequently, the PI controller will reduce the MR damper control current from i_1 to i_2 so that the MR damper resistance force F_a can approach the desired result F_a^*.

In scenario 2, the relative velocity across MR damper d_s is $\dot{\delta}_b < 0$. But, the control error $e(t) = F_b^* - F_b > 0$. In this case, the output of the sign block is -1, $\bar{e}(t) = -e(t) = -F_b^* + F_b < 0$. Consequently, the PI controller will again reduce the MR damper control current from i_1 to i_2 so that the MR damper resistance force F_b can approach the desired result F_b^*. Clearly, in this scenario, without the sign block, the situation will be just the opposite.

References

[1] Mead D J 1998 *Passive Vibration Control* (New York: Wiley)

[2] Daley S, Johnson F A, Pearson J B and Dixon R 2004 Active vibration control for marine applications *Control Eng. Prac.* **12** 465–74

[3] Winberg M, Crolla D A and Plummer A R 2005 Active vibration isolation in ships: a pre-analysis of sound and vibration problems *Int. J. Acoust. Vib.* **10** 175–96

[4] Olsson C 2006 Active automotive engine vibration isolation using feedback control *J. Sound Vib.* **294** 162–76

[5] Guclu S 2005 Fuzzy logic control of seat vibrations of a non-linear full vehicle model *Nonlinear Dyn.* **40** 21–34

[6] Crede C E and Ruzicka J E 2002 Theory of vibration isolation *Shock and Vibration Handbook* 5th edn (New York: McGraw-Hill)

[7] Brennan M J and Ferguson N S 2004 *Vibration Control Advanced Applications in Acoustics Noise and Vibration* (London: E&FN SPON)

[8] Ruzicka J E and Derby T E 1971 *Influence of Damping in Vibration Isolation* T.S.a.V.I Centre US Department of Defence

[9] Lang Z Q, Jing X J, Billings S A, Tomlinson G R and Peng Z K 2009 Theoretical study of the effects of nonlinear viscous damping on vibration isolation of sdof vibrating systems *J. Sound Vib.* **323** 352–65

[10] Laalej H, Lang Z Q, Daley S, Zazas I, Jing X J, Billings S A and Tomlinson G R 2011 Application of non-linear damping to vibration isolation: an experimental study *Nonlinear Dyn.* doi:10.1007/s11071011-0274-1

[11] Peng Z K, Lang Z Q, Zhao L, Guo P F, Billings S A and Tomlinson G R 2011 The force transmissibility of MDOF structures with a nonlinear viscous damping device *Int. J. Nonlinear Mech.* **46** 1305–14

[12] Nevala K and Jarviluoma M 1997 An active vibration damping system of a driver's seat for off-road vehicles *Proc. Mechatronics and Machine Vision in Practice (Toowoomba)* pp 38–43

[13] Stayner R M, Hilton D J and Moran P 1975 Protecting the tractor driver from low frequency ride vibration *Proc. Institution of Mechanical Engineers CP* 11/75

[14] Burdorf A and Swuste P 1993 The effect of seat suspension on exposure to whole body vibrations of professional drivers *Ann. Occup. Hygiene* **37** 45–55

[15] Choi S B, Nam M H and Lee B K 2000 Vibration control of a MR seat damper for commercial vehicles *J. Intell. Mater. Syst. Struct.* **11** 936–44

[16] Metered H, Bonello P and Oyadiji S O 2009 Vibration control of a seat suspension system using magnetorheological damper *IDETC/CIE2009: Int. Design Engineering Technical Conf. and Computers and Information in Engineering Conf. (San Diego, CA, Aug.–Sept.)*

[17] Sapinski B 2005 Fuzzy control for MR damper in a driver's seat suspension *J. Theor. Appl. Mech.* **43** 179–201

[18] Chang C C and Zhou L 2002 Neural network emulation of inverse dynamics for a magnetorheological dampers *J. Struct. Eng.* **128** 231–9

[19] Zhou L and Chang C C 2003 Adaptive fuzzy control for nonlinear building—magnetorheological damper system *J. Struct. Eng.* **129** 905–13

[20] Dyke S J, Spencer B F, Sain M K and Carlson J D 1996 Modeling and control of magnetorheological dampers for seismic response reduction *J. Smart Mater. Struct.* **5** 565–75

[21] Sims N D, Stanway R, Johnson A R, Peel D J and Boullough W A 2000 Smart fluid damping: shaping the force/velocity response through feedback control *J. Intell. Mater. Syst. Struct.* **11** 945–9

[22] Song X, Ahmadian M and Southward S C 2005 Modeling magnetorheological dampers with application of

nonparametric approach *J. Intell. Mater. Syst. Struct.* **16** 421–32

[23] Shames I H and Cozzarelli F A 1992 *Elastic and Inelastic Stress Analysis* (Englewoods Cliffs, NJ: Prentice Hall) pp 120–2

[24] Spencer B F, Dyke S J, Sain M K and Carlson J D 1997 Phenomenological model of a magnetorheological damper *J. Eng. Mech., ASCE* **123** 230–8

[25] Wen Y K 1976 Method of random vibration of hysteretic systems *J. Eng. Mech. Div. ASCE* **102** 249–63

[26] Hsu J C and Meyer A U 1968 *Modern Control Principles and Applications* (New York: Mc Graw-Hill) pp 116–20

[27] McClamroch N H and Gavin H P 1995 Closed loop structural control using electroheological dampers *Int. Proc. American Control Conference* vol 6 *(Seattle, WA)* pp 4173–7

[28] Cebon D, Besinger F H and Cole D J 1996 Control strategies for semi-active lorry suspensions *Proc. Inst. Mech. Eng.* D **210** 161–78

[29] Simon D and Ahmadian A 2001 Vehicle evaluation of the performance of magneto rheological dampers for heavy truck suspensions *J. Vib. Acoust.* **123** 365–75

[30] Lang Z Q, Billings S A, Yue R and Li J 2007 Output frequency response function of nonlinear Volterra systems *Automatica* **43** 805–16

[31] Guo P F and Lang Z Q 2011 Nonlinear viscous damping design for civil structure vibration control using output frequency response function *Proc. 2011 World Congr. on Advances in Structural Engineering and Mechanics* pp 2235–56

[32] Sapinski B and Rosol M 2008 Autonomous control system for a 3 DOF pitch-plane suspension model with MR shock absorber *Comput. Struct.* **86** 379–85